3-D core modelling of RIA transient: the TMI-1 benchmark

P. Ferraresi[*], E. Studer[**], A. Avvakumov[***], V. Malofeev[***], D. Diamond[****], B. Bromley[****]

[*]*Institut de protection et de sûreté nucléaire, Département de Recherches en Sécurité, CEA Cadarache - 13108 ST Paul-lez-Durance*
[**]*Direction des Etudes Nucléaires, Département de Modélisation des Systèmes et des Structures, CEA Saclay - 91191 Gif sur Yvette - France*
[***]*Nuclear Safety Institute of Russian Research Center "Kurchatov Institute, Kurchatov square 1 - Moscow - Russia*
[****]*Nuclear Energy & Infrastructure Systems Division, Brookhaven National Laboratory - BNL 130 – Upton - NY 11973-5000 - USA*

Abstract: The increase of fuel burn up in core management poses actually the problem of the evaluation of the deposited energy during Reactivity Insertion Accidents (RIA). In order to precisely evaluate this energy, 3D approaches are used more and more frequently in core calculations. This "best-estimate" approach requires the evaluation of code uncertainties. To contribute to this evaluation, a code benchmark has been launched. A 3D modelling for the TMI-1 central Ejected Rod Accident with zero and intermediate initial powers was carried out with three different methods of calculation for an inserted reactivity respectively fixed at 1.2 $ and 1.26 $. The studies implemented by the neutronics codes PARCS (BNL) and CRONOS (IPSN/CEA) describe an homogeneous assembly, whereas the BARS (KI) code allows a pin-by-pin representation (CRONOS has both possibilities).

All the calculations are consistent, the variation in figures resulting mainly from the method used to build cross sections and reflectors constants. The maximum rise in enthalpy for the intermediate initial power (33 % P_N) calculation is, for this academic calculation, about 30 cal/g. This work will be completed in a next step by an evaluation of the uncertainty induced by the uncertainty on model parameters, and a sensitivity study of the key parameters for a peripheral Rod Ejection Accident.

1. INTRODUCTION

One of the major issue related to the increase of core fuel burn up is the evaluation of the deposited energy in the event of a rod ejection accident in a PWR or a rod drop accident in a BWR, and the evaluation of acceptable safety limits. Rather than using conservative 1D-2D methodologies for core calculation, as it is currently the case, advanced studies use more and more 3D "best-estimate" approaches which must take into account uncertainties involved with the method.

One of the sources of uncertainty is the fuel pin representation, the fuel assembly being described, in the majority of the codes, in a homogeneous way; not taking into account the inter-assembly can lead to a rather important underestimation of the fuel enthalpy.

Collaboration between the US NRC (U. S. Nuclear Regulatory Commission) and the RRC-KI (Russian Research Center – Kurchatov Institute) has been initiated, with the participation of the IPSN (Institut de Protection et de Sûreté Nucléaire), and will concentrate on the neutronics aspect of reactivity accidents.
The aim is to improve knowledge on uncertainties in "best-estimate" 3 dimensional calculations for rod ejection accident, comparing results obtained by three different neutronics codes. PARCS [1], used by BNL, gives a homogeneous representation of the fuel assembly and is completed by a method of flux
reconstruction (reconstitution of the power distribution pin by pin). BARS [2], developed by RRC-KI, explicitly describes the fuel pins. CRONOS2 [3], carried out by the CEA, provides both a
homogeneous or heterogeneous description of a fuel assembly, from nuclear libraries supplied or built with APOLLO2 [4] and the corresponding isotopic compositions.

It is important to notice that this project, entrusted by NRC to BNL (Brookhaven National Laboratory), constitutes more an exercise in code comparison than a reference case. Moreover, the description of the transient requires a coupling between neutronics and thermal-hydraulics. The thermal-hydraulic codes used are RELAP5 [5] for BNL and KI (two-phase 1D with description of one channel by assembly), FLICA4 [6], [7], [8] for the IPSN/CEA (two-phase 3D with description of one or more channels by assembly, and possibility of fuel cell channel representation).

This exercise concerns a PWR at the end of cycle. The selected reactor is the Three Mile Island Unit 1, which has already been the subject of an international study [9], and for which participants had access to public data, especially nuclear libraries with 2 energy groups. Calculations simulate a central rod ejection accident transient without reactor trip.

2. DESCRIPTION OF THE EXERCISE

The choice of a central rod ejection, with inserted regulation banks, allows a 1/8th symmetry of TMI-1 core. The fuel burnup rates of the various assemblies differ from 23 to 58 GWd/t, an average radial burnup rate being considered for each assembly. Moreover, the assembly is divided axially into 15 layers with different burnups. All neutronic and thermal-hydraulic data, as well as isotopic compositions [10], have been provided by the American partners.

All participants carried out a 3D diffusion calculation with 2 energy groups. With regard to NRC and the IPSN/CEA, the isotopic compositions and the reflectors constants are identical, and they are assembly averaged with the American CASMO-3 code [11]. On the other hand, those used by KI [12], pin averaged, are built with the TRIFON code [13] from material balances. All of these libraries come from basic values included in the international data library ENDF/B [14], [15].

The accident is initiated from a critical core at zero power and is characterized by the ejection of the central rod in 100 ms. The rods of the regulation banks (5, 6 and 7) are fully inserted in the core. The transient is completed in 2.5 s, without taking reactor trip into account. In order to reach over-criticality, and to ensure a comparison of the results, the ejected rod worth is initially fixed, by participants, at 1.2 $. The core, which fuel assemblies have varying burnup rates from 23 to 58 GWd/t, has a 1/8th symmetry, as shown in figure 1, and the regulation banks are close to the assemblies with high burnup.

Initially, the core power is 10^{-6} P_N (with P_N = 2772 MW), the pressure is 151.68 bars, the average moderator temperature is 551 K, the water density is 0.7695 g/cc, the fuel temperature is 551 K, and the boron mass concentration is 5 ppm. The fraction of delayed neutrons is considered to be uniform for the whole core (β = 521 pcm).

The exercise also envisages a sensitivity study with an initial power of 33 % P_N.

3. COMPARAISON OF RESULTS AT ZERO INITIAL POWER

3.1 Steady state

Before being implemented, the calculation methods are adjusted based on a series of stationary configurations [16]. Table 1 presents the synthesis of a number of characteristic parameters calculated by the three partners, as well as the corresponding variations.
Figures 2 and 3 show the comparison between the predictions of the three partners concerning the averaged radial assembly power distribution and the axial core distribution.
Stationary study results confirm the consistency between the various codes. The banks worth values, as those of the temperature coefficients, are very close to each other (deviation stay below 10 %).The control rods worth is also consistent, except in the case of the rod of the "N12" assembly, close to the reflector, for which BARS over-estimates its value by approximately 37 %. A first calculation with BARS, based on other reflectors constants, gave a variation on this variable of about 58 %, showing the high influence of reflectors modelling on this result. Furthermore, with regards to the radial distribution of the averaged assembly power, it is clear that PARCS and CRONOS are comparable codes, with variations being everywhere lower than 1 %. BARS, which presents variations lower than 6 %, underestimates the power in the central assembly by 5.6 %. The axial power distribution is identical for the three calculations.

However, the variations obtained with BARS can be explained by the different cross sections and reflectors constants, which are more difficult to precisely calculate in the strong flux distortion zones, such as barred cells close to the reflectors.

3.2 Transient

The basic scenario is based on a fast ejection of the central control rod which worth is fixed at 1.2 $, the fraction of delayed neutrons being 521 pcm. It is interesting to recall that, for thermal-hydraulics transient, BNL and KI use the same RELAP5 code, whereas the IPSN/CEA carries out the coupling with the FLICA4 code.

The results, summarized in table 2, illustrate a good consistency between the three methods of calculation. The peak power obtained by CRONOS appears later and is slightly underestimated compared to that of PARCS. This can be explained by a lower ejected rod worth of approximately 2%, which obviously modifies the kinetics of the transient (pulse half width of 70 ms with CRONOS instead of 63 ms with PARCS and BARS). The hottest assembly "H9", identical for all of the partners, is the closest assembly to the central one, containing the ejected rod and having a low burnup. The peak of axial power is located in the same location at the top of the hottest assembly.

The transient core power behavior versus time is represented in figure 4. Peaks reach values close to 4 times the nominal power, leading to approximately 11 GW.

The different contributions to the reactivity versus time obtained by CRONOS during the transient are plotted in figure 5. The global reactivity, which grows for 100 ms until reaching the inserted reactivity (1.2 $), falls at around 290 ms, when the Doppler feedback becomes significant. This decrease is accelerated in the following milliseconds (~ 50 ms) by the moderator effect. This phenomenon intervenes at a very early stage because of an extremely fast heat transfer between the fuel and the moderator. Moreover, it should be noted that all the reactivity feedback occurs, in the case of a transient at zero initial power, after the complete central rod ejection.

The averaged radial assembly power distributions are illustrated in figure 6 for 1/8th of the core, at the time of maximum power and at the end of the calculation. The maximum power, after the central rod ejection, is reached in the closest less irradiated assembly to the one which contains the ejected rod. However, power redistribution at the hot point is not simply confined to the center of the core. It extends over several assemblies rows and more precisely to the assemblies with a low burnup, thus close to the control rods. Power decreases by approximately 22 % in the “K10” assembly which is the hottest after “H9”.

The major differences, although low, are observed in the case of the BARS calculations and are mainly a consequence of the different origins of the cross sections and reflectors [17], [18], [19], constants, as mentioned in §2.

All results are obtained with a thermal-hydraulic description based on an averaged assembly. A study carried out with FLICA4 [20], which divides the assembly into four channels, did not show any significant improvement.
It should be noted that a pin-by-pin flux reconstruction method was developed by BNL from the assembly average values. The Kurchatov Institute showed that satisfying results were obtained for this transient with regards to the radial power distribution, as well as fuel temperature [21], [22]. The comparison enhances the slight conservatism of a “coarser” approach (temperature average on an assembly) compared to a finer method (pin-by-pin thermics), for instance, less than 2 % deviation for peak power and maximum fuel enthalpy increment, and 0.1 K for fuel pin temperature.

The three calculations, illustrated in figure 7, lead fuel enthalpy rises for the hottest averaged assembly of the same order of magnitude, approximately 20 cal/g. The hottest pellet, as calculated by BARS, is located in the hottest assembly. Its enthalpy rise is about 21 cal/g. Maxima fuel enthalpy and enthalpy rise are obtained at 2.5 s (the end of the calculation).

4. EFFECT OF INITIAL CORE POWER

In the previous paragraphs, ejection of the central control rod in the TMI-1 PWR at zero power operating conditions (10^{-6} nominal power – HZP) has been described and analyzed. At this power level, feedback effects appear after the ejection of the control rod. Unlike a zero power case, in the non-zero power conditions, the fuel is thermally active at the beginning of the transient and feedback effects appear during the ejection of the control rod.

In order to investigate the effects of initial core power on the key safety parameters, calculations have been carried out at 33 % nominal power using RELAP/BARS [23], PARCS stand-alone (with its own thermal-hydraulics solver) and SAPHYR (CRONOS2/FLICA4). The banks 5 and 7 are fully inserted and in both calculations (BARS and CRONOS), the ejected control rod worth is fixed to 1.26 β in order to reach the same maximum value for the reactivity (about 1.2 β) and to simplify the comparison with the zero power calculations. To reach criticality at the initial steady state, an additional withdrawal of control rods at the core periphery (BARS) or a renormalization of the fission matrices with k_{eff} value (CRONOS) is carried out. In the PARCS calculation, the ejected control rod worth is about 1.2 β. For the three calculations, the initial conditions are not exactly the same (BARS and CRONOS are close together while PARCS data are slightly different) and for comparison, only limited conclusions can be drawn.

Figures 8 and 9 show the reactor power and the reactivity during the transient. The reactor power reaches a maximum value of 10 to 14 times the nominal power, mainly depending on different control rod worths and different Doppler reactivity coefficient (the smallest corresponds to BARS calculation).
Figure 10 shows the maximum fuel enthalpy rise in the hottest fuel pellet (BARS) and in the hottest fuel assembly (PARCS and CRONOS) versus time. These results concern the fuel assembly “H9” and the main differences correspond to the different injected energy (figure 8: reactor power versus time). As for the maximum enthalpy rise in the hottest fuel assembly, differences between the three calculations are about 10 %, and this value is obtained at the end of the transient in fuel assembly “H9”. Unlike enthalpy rise, the maximum fuel enthalpy is calculated in the fuel assembly “K10” and this maximum value is obtained in about 0.4-0.6 s.
Figure 11 shows averaged assembly radial power at three different stages during the transient (initial state, time of peak power, and end of the transient). Unlike zero power initial conditions, significant deformations in the radial power distribution take place after the control rod ejection, mainly due to moderator effect. The maximum evolution of assembly power between the time of peak power and the end of the transient is reached in the assembly “H8”. This corresponds to a variation of 14.6 % with BARS, 16.3 % with CRONOS (deformations quite similar), and 19.1 % with PARCS calculation.

Key safety parameters are summarized in table 3. The increase in the maximum fuel enthalpy increment is 24-29 cal/g with intermediate initial power (33 % P_N) as compared to17-20 cal/g in the zero power initial (HZP) conditions, leading to a difference of about 40-45 %. The maximum fuel pellet enthalpy reaches 60-67 cal/g as compared to 34-37 cal/g in the HZP case (difference of 75-80 %).

5. CONCLUSIONS

This study confirms the consistency between the various methods for 3D calculations which have been used during a central Rod Ejection Accident in a PWR at the end of the cycle.

Results at zero initial power are very similar, however it should be noted that the variations are more significant with a higher gradient of power in the assembly, as calculations at intermediate power show. The maximum fuel enthalpy rise is higher than that in the HZP calculation (45 %) as well as the maximum enthalpy (~ 80 %).

The flux reconstruction method developed by BNL provides satisfactory results. The calculation assumptions with homogenization of the assembly are, for this study, slightly conservatory. Although they cannot account for the enthalpy increase in the hottest pellet under all circumstances (the latter not being inevitably in the hottest assembly), the variations observed, for a comparable ejected rod worth, come in majority from the cross sections and reflectors constants preparation method, rather than from a geometrical discretisation and/or an intra-assembly representation.

However, it should be noted that this exercise is based on academic cases. Indeed, it does not seem very realistic to consider a management that would lead to a transient of ejected rod accident likely to insert such important reactivity (1.26 $) especially from an initial power of 33 % P_N.

The 3D “best-estimate” approach used in this study should be completed by an evaluation of the results uncertainties induced by modelling and input parameters uncertainties. This point will be the subject of the next step of this study. In the same way, a sensitivity study of the key parameters will be taken into account for the more delicate exercise of rod ejection accident in the periphery of the core, therefore close to the reflector.

REFERENCES

1. H. G. Joo, et al., “PARCS : a Multi-Dimensional Two-Group Reactor Kinetics Code Based on the Non-linear Analytic Nodal Method”, PU/NE-98-26. Purdue University, September 1998
2. A. Avvakumov, and V. Malofeev, “An Advanced 3D Pin-by-Pin Neutronic Model for LWR Detailed Pin-by-Pin Calculations”, Proceedings of the international Conference on the Physics of Nuclear Science and Technology, Long Island, NY, October 1998
3. J.-J. Lautard, S. Loubière, C. Fedon-Magnaud, “CRONOS2 a Modular Computational System for Neutronic Core Calculations”, IAEA Specialist Meeting on Advanced Calculations Methods for Power Reactors, Cadarache (France), 1990
4. S. Loubière, M. Coste, Z. Stankovski, I. Zmijare, R. Sanchez, A. Hebert, C. Van Der Gucht, “APOLLO2 twelve years later”, NT SERMA/LENR/PU/99-2557/B
5. “RELAP5/MOD3.2 Code Manual”, NUREG/CR-5535, INEL-95/0174, 1995
6. I. Toumi, D. Gallo, A. Bergeron, E. Royer. “Advanced Numerical Methods for three Dimensional two-phase flow Calculations in PWR”, NURETH-8 Meeting, Kyoto (Japan), 1997
7. I. Toumi, A. Bergeron, D. Gallo, E. Royer, D. Caruge, “FLICA-4 : a three-Dimensional two-Phase Flow Computer Code with Advanced Numerical Methods for Nuclear Applications”, Nuclear Engineering and Design, 200 (2000) 139-155, 2000
8. E. Royer, I. Toumi, “CATHARE-CRONOS-FLICA, coupling with ISAS: a Powerful TOOL for Nuclear Studies, ICÔNE-6 Meeting, San Diego (USA), 1998
9. K. N. Ivanov , et al., “Pressurized Water Reactor Main Steam Line Break (MSLB) Benchmark ; Volume 1 : Final Specifications”, NEA/NSC/DOC(99)8, U.S. Nuclear Regulatory Commission and OECD Nuclear Energy Agency, April 1999
10. P. Ferraresi, C. Gouin, “TMI-1 RIA Benchmark Data (Rev 0)”, MEMO SEMAR 98/30, November 1998
11. D. J. Diamond, et al., “Intercomparison of Results for a PWR Rod Ejection Accident”, Proceedings of the International Twenty-Seventh Water Reactor Safety Information Meeting, Bethesda, Maryland, October 1999
12. A. Avvakumov, et al., “Validation of the BARS Code Package with ENDF/B Based Data Library”, Report N° 90-12/1-4-98, Nuclear Safety Institute of Russian Research Center Kurchatov Institute, 1998
13. A. Kwaratzhely, and B. Kochurov, “A Method for Calculation of Neutronic Parameters in a Heterogeneous Reactor Cell”, At. Energy, 58(2), 1985
14. P. F. Rose, Ed., “ENDF/B Summary Documentation”, BNL-NCS-17541 (ENDF-201, 4th ed. (ENDF/B-VI), Brookhaven National Laboratory, October 1991 ; Release-2, 1993 ; Release-3, 1996
15. R. E. McFarlane, “NJOY91.91 : A Code System for Producing Pointwise and Multigroup Neutron and Photon Cross Sections from ENDF/B Evaluated Nuclear Data”, ORNL PSR-171, Oak Ridge National Laboratory, 1993
16. C. Gouin, P. Ferraresi, M. Rohart, E. Royer, “Benchmark TMI-1 : Synthesis of Stationary Results”, NT SEMAR 99/125, July 2000
17. S. Aniel-Buchheit, “Progress in Works concerning the 3-D Modelisation for the RIA in TMI-1”, Report DMT-SERMA/LCA/RT/00-2773/B, November 2000
18. S. Aniel-Buchheit, “Creation and Analyses of Homogeneous and Heterogeneous Libraries for the Reactor TMI-1 : Benchmark TMI-1”, Report DMT-SERMA/LCA/00-2814/A, November 2000
19. S. Aniel-Buchheit, “Reflector Data Construction for the Reactor TMI-1 (Benchmark TMI-1)”, Report DMT-SERMA/LCA/RT/00-2782/A, October 2000
20. E. Studer, J. C. Lepallec, P. Ferraresi, “RIA Modelling in TMI-1. Physical Analysis from Central Rod Ejection Results at Zero Power”, Report DM2S, SERMA draft, 2001

21. A. Avvakumov, V. Malofeev, and V. Sidorov, “Analysis of Pin-by-Pin Effects for LWR Rod Ejection Accident”, NUREG/IA-0175, NSI RRC KI90-12/1-3-00, IPSN/00-13, March 2000

22. V. Malofeev, “Effect of Detailed Intra-assembly Fuel Temperature Representation on the Course of the TMI-1 Ejection Accident”, US NRC-IPSN-RRCKI Meeting, Washington, October 1999
23. A. Avvakumov, V. Malofeev, and V. Sidorov, “Uncertainty Analysis for the PWR Rod Ejection Accident Using the RELAP-BARS Code”, NSI-RRC-KI 90-12/1-1-01

Table 1: comparison of steady state results

Reference case → core at Hot Zero Power [$P = 10^{-6} P_N$; inserted rods (5, 6, 7), $T_{mod} = T_{fuel}$ = 551 K]

In brackets → authorised discrepencies

In bold type → IPSN-CEA/BNL, KI/BNL deviations

Parameters	BNL	KI	IPSN/CEA
k_{eff} for the reference case (pcm) (HZP)	1,00187 (± 1000 pcm)	1,00203 **- 39 pcm**	1,00165 **- 22 pcm**
Worth of bank 5 (pcm)	1423 (± 15 %)	1532 **7,6 %**	1427 **0,3 %**
Worth of bank 6 (pcm)	848 (± 15 %)	856 **9,4E-5 %**	848 **0 %**
Worth of bank 7 (pcm)	1049 (± 15 %)	1083 **3,2 %**	1048 **- 0,1 %**
Worth of central rod (H8) (pcm) Inserted banks	346	349 **1,2 %**	345 **- 0,29 %**
Worth of rod H12 (pcm) Inserted banks	188	204 **8,2 %**	188 **0 %**
Worth of rod N12 (pcm) Inserted banks	345	473 **37 %**	353 **2,3 %**
Doppler coefficient (pcm/K)	Not calculated	- 2,81	- 2,80
Isothermal coefficient (pcm/K)	- 47,90 (± 4 pcm/K)	- 46,80 **1,9 pcm/K**	- 47,54 **0,4 pcm/K**
Power coefficient (pcm)	2382 (± 10 %)	2230 **-6,2 %**	2365 **- 0,7 %**

Table 2 : comparison of parameters during the HZP transient

Parameter	NRC	KI	IPSN/CEA
Maximum inserted reactivity (β)	1.222	1.209	1.199
Peak poer of the core (GW)	10.73	10.69	10.17
Time of peak power (ms)	342	338	363
Power pulse width (ms)	63	63	70
Position of the hottest assembly	H9	H9	H9
Maximum fuel "assembly H9" enthalpy (cal/g)	33.84	37.60	35.99*
Maximum fuel "assembly" enthalpy increment (cal/g)	17	19	18.58
Maximum fuel "pellet" enthalpy increment (cal/g)	-	20.6	-

* This fuel enthalpy value takes into account an initial enthalpy at 20 °C of 1 ($H_{calculation}$ + 1)

Table 3 : comparison of parameters during the 33% PN of initial power transient

Parameter	33%Pn RELAP/BARS	33%Pn PARCS	33%Pn SAPHYR
Maximum inserted reactivity (β)	1.220	1,212	1.238
Core peak power (%Pn/GW)	1397 / 38.7	1014 / 28.1	1201 / 33.3
Time of peak power (ms)	130	136	133
Power pulse width (ms)	44	48	43
Position of the hottest assemblies	K10 and H9	H9 and K10*	K10 and H9
Maximum fuel pellet enthalpy (cal/g)	66.7 (K10)	59.6 (H9)	65.6 (K10)**
Time of maximum fuel enthalpy (ms)	~ 50	~ 65	~ 55
Maximum fuel pellet enthalpy rise at 2.5 s (cal/g)	28.7 (H9)	24.3 (H9)	25.2 (H9)

* Fuel assembly hot spot ** Average fuel pin

	8	9	10	11	12	13	14	15
H	52.86 Bank 7	30.19	56.25	30.85	49.53 Bank 7	28.11	53.86 Bank 6	55.78
K		57.94	30.80	55.43	29.83	53.95 Bank 5	25.55	49.17
L			57.57 Bank 6	30.22	54.40	27.86	23.30	47.30
M				49.71 Bank 5	28.85	52.85	40.94	
N					48.75 Bank 7	23.86	41.45	
O						37.34		

Fuel Burnup (GWd/t)
N°. of regulating bank

Figure 1 : one-eight core layout

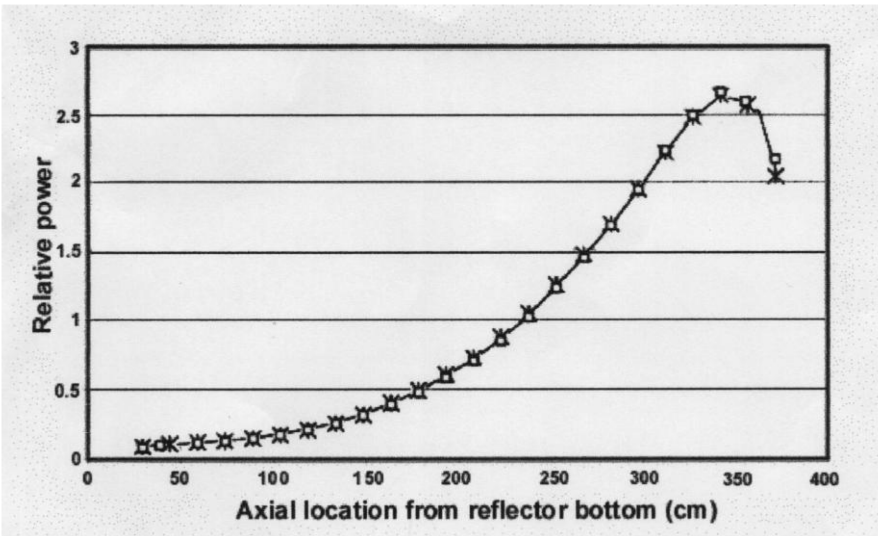

— CRONOS * PARCS o BARS

Figure 2 : axial power distribution at initial conditions

	8	9	10	11	12	13	14	15
H	0,916 0,921 0,869	1,865 1,875 1,790	1,570 1,576 1,515	1,591 1,598 1,557	0,663 0,665 0,647	0,842 0,846 0,820	0,387 0,386 0,383	0,284 0,284 0,274
K		1,513 1,519 1,447	1,715 1,723 1,662	1,278 1,281 1,250	1,246 1,250 1,247	0,613 0,613 0,618	0,933 0,929 0,961	0,388 0,386 0,390
L			0,817 0,820 0,787	1,319 1,324 1,307	1,099 1,100 1,165	1,318 1,314 1,371	1,115 1,107 1,162	0,402 0,400 0,411
M				0,675 0,676 0,668	1,244 1,244 1,255	1,060 1,055 1,078	0,794 0,790 0,816	
N					0,728 0,726 0,709	1,150 1,144 1,155	0,538 0,536 0,538	
O						0,663 0,660 0,667		

CRONOS
PARCS
BARS

	8	9	10	11	12	13	14	15
H	- 0,5 % - 5,6 %	- 0,5 % - 4,5 %	- 0,4 % - 3,9 %	- 0,4 % - 2,5 %	- 0,4 % - 2,7 %	- 0,4 % - 3,1 %	+ 0,3 % - 0,8 %	+ 0,2 % - 3,5 %
K		- 0,4 % - 4,7 %	- 0,5 % - 3,5 %	- 0,2 % - 2,4 %	- 0,3 % - 0,2 %	+ 0,1 % + 0,8 %	+ 0,4 % + 3,4 %	+ 0,5 % + 1,0 %
L			- 0,4 % - 4,0 %	- 0,4 % - 1,3 %	- 0,1 % + 5,9 %	+ 0,3 % + 4,3 %	+ 0,7 % + 5,0 %	+ 0,6 % + 2,7 %
M				- 0,1 % - 1,2 %	0 % + 0,9 %	+ 0,5 % + 2,2 %	+ 0,5 % + 3,3 %	
N					+ 0,2 % - 2,3 %	+ 0,5 % + 1,0 %	+ 0,4 % + 0,4 %	
O						+ 0,4 % + 1,1 %		

CEA/BNL
KI/BNL

Figure 3 : radial assembly averaged power distribution at initial conditions

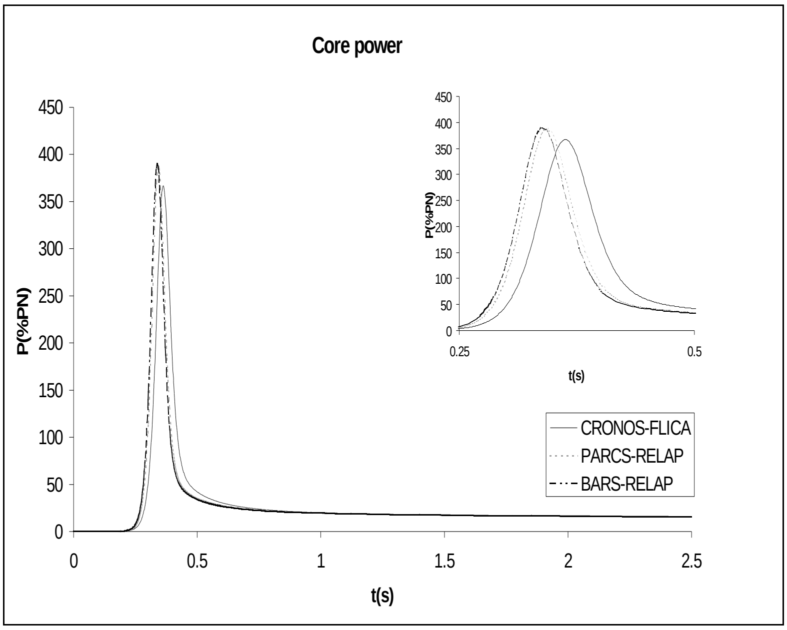

Figure 4 : core power distribution

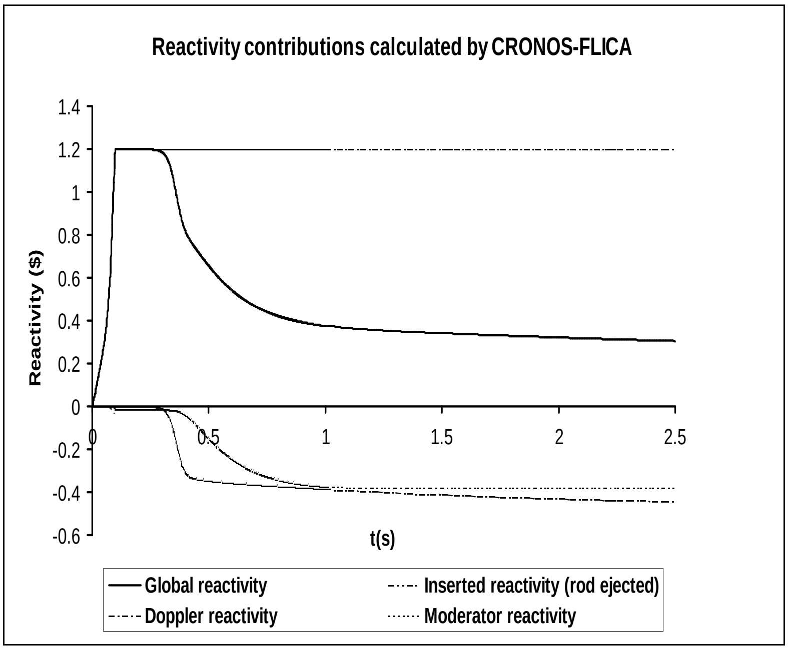

Figure 5 : reactivity contributions

	8	9	10	11	12	13	14	15
H	2.052 2.051 2.066	2.614 2.615 2.626	1.871 1.870 1.854	1.721 1.724 1.708	0.6631 0.6646 0.6490	0.7841 0.7879 0.7570	0.3449 0.3452 0.3370	0.2483 0.2489 0.2360
K		1.963 1.961 1.947	1.995 1.997 1.980	1.354 1.354 1.337	1.222 1.226 1.222	0.5635 0.5640 0.5620	0.8232 0.8225 0.8360	0.3376 0.3371 0.3340
L			0.8930 0.8945 0.8730	1.331 1.335 1.320	1.038 1.038 1.092	1.183 1.181 1.216	0.9766 0.9722 1.0030	0.3489 0.3484 0.3520
M				0.6449 0.6461 0.6340	1.130 1.132 1.129	0.9344 0.9319 0.9390	0.6899 0.6883 0.7000	
N					0.6429 0.6422 0.6180	0.9976 0.9948 0.9870	0.4641 0.4630 0.4570	
O						0.5703 0.5692 0.5650		

Time of maximum power : tmax

	8	9	10	11	12	13	14	15
H	1.916 1.915 1.926	2.450 2.452 2.464	1.777 1.777 1.757	1.666 1.670 1.647	0.6595 0.6610 0.6410	0.8026 0.8062 0.7740	0.3598 0.3599 0.3520	0.2613 0.2617 0.2490
K		1.849 1.848 1.831	1.905 1.909 1.885	1.319 1.320 1.297	1.221 1.224 1.218	0.5782 0.5784 0.5760	0.8589 0.8578 0.8760	0.3554 0.3547 0.3530
L			0.8684 0.8702 0.8410	1.318 1.322 1.302	1.047 1.047 1.103	1.218 1.216 1.257	1.018 1.013 1.053	0.3671 0.3664 0.3720
M				0.6515 0.6526 0.6380	1.158 1.159 1.158	0.9675 0.9645 0.9760	0.7213 0.7195 0.7350	
N					0.6664 0.6653 0.6420	1.041 1.038 1.037	0.4877 0.4864 0.4830	
O						0.5987 0.5974 0.596		

Final time : 2.5 s

CRONOS PARCS BARS

Figure 6 :   radial assembly averaged power distributions versus time

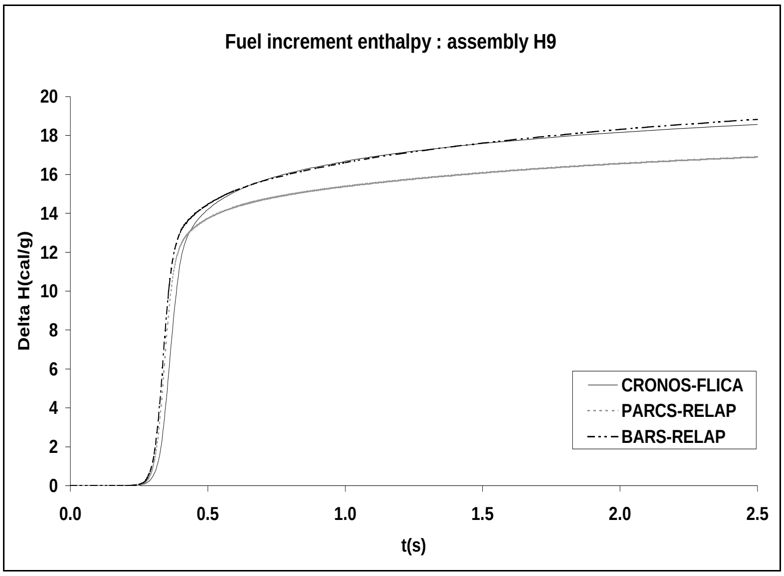

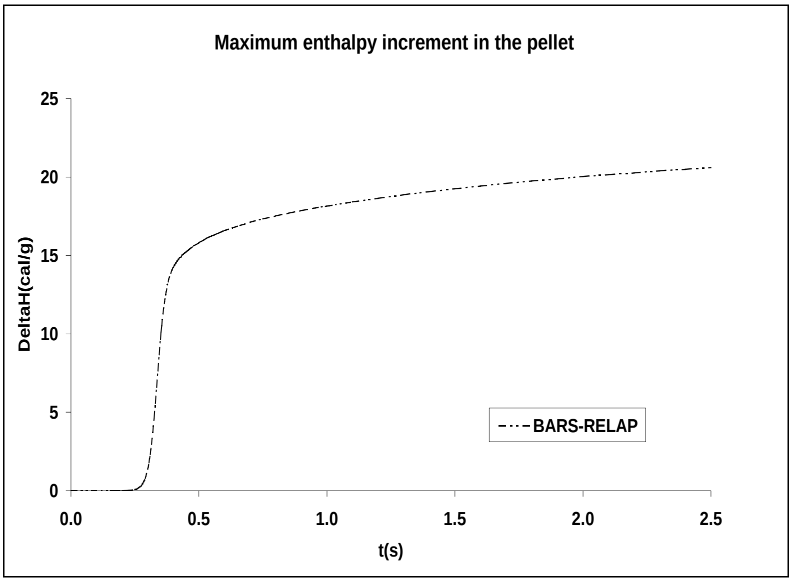

Figure 7 : fuel assembly and pellet enthalpy increment

Figure 8 : reactor power versus time

Titre :
reac33.eps
Auteur :
studer@finlay with xmgr
Aperçu :
Cette image EPS n'a pas été enregistrée
avec un aperçu intégré.
Commentaires :
Cette image EPS peut être imprimée sur une
imprimante PostScript mais pas sur
un autre type d'imprimante.

Figure 9: reactivity versus time

Titre :
dh33.eps
Auteur :
studer@finlay with xmgr
Aperçu :
Cette image EPS n'a pas été enregistrée
avec un aperçu intégré.
Commentaires :
Cette image EPS peut être imprimée sur une
imprimante PostScript mais pas sur
un autre type d'imprimante.

Figure 10: maximum fuel enthalpy increment versus time

	8	9	10	11	12	13	14	15
H	0.213	1.169	1.298	1.458	0.647	0.974	0.747	0.391
	1.936	2.514	1.826	1.687	0.641	0.830	0.589	0.299
	1.690	2.227	1.654	1.580	0.636	0.878	0.646	0.333
K		1.139	1.613	1.242	1.247	0.664	1.141	0.471
		1.936	2.133	1.383	1.202	0.561	0.893	0.361
		1.726	1.949	1.305	1.202	0.595	0.984	0.402
L			1.278	1.445	1.157	1.355	1.189	0.438
			1.502	1.495	1.051	1.112	0.927	0.334
			1.398	1.443	1.071	1.191	1.021	0.372
M				0.704	1.217	1.021	0.785	
				0.665	1.040	0.817	0.608	
				0.669	1.091	0.883	0.671	
N					0.664	1.062	0.499	
					0.537	0.826	0.383	
					0.579	0.908	0.424	
O		T = 0 s				0.607		
		T = 0.130 s				0.464		
		T = 2.5 s				0.514		

Assembly Averaged Power at three states of the core (BARS)

	8	9	10	11	12	13	14	15
H	0.253	1.236	1.337	1.483	0.664	0.991	0.746	0.400
	1.947	2.508	1.832	1.694	0.657	0.855	0.598	0.312
	1.635	2.171	1.653	1.596	0.654	0.902	0.652	0.345
K		1.188	1.638	1.259	1.244	0.663	1.106	0.472
		1.943	2.120	1.390	1.202	0.566	0.880	0.367
		1.713	1.934	1.321	1.203	0.600	0.963	0.407
L			1.299	1.442	1.092	1.310	1.148	0.434
			1.508	1.488	0.998	1.088	0.907	0.367
			1.413	1.450	1.020	1.162	0.998	0.374
M				0.712	1.216	1.015	0.776	
				0.673	1.046	0.821	0.609	
				0.682	1.099	0.887	0.670	
N					0.694	1.080	0.513	
					0.567	0.850	0.398	
					0.612	0.933	0.441	
O		T = 0 s				0.621		
		T = 0.136 s				0.481		
		T = 2.5 s				0.533		

Assembly Averaged Power at three states of the core (PARCS)

	8	9	10	11	12	13	14	15
H	0.224	1.261	1.394	1.505	0.698	0.967	0.742	0.384
	2.030	2.553	1.888	1.703	0.686	0.829	0.591	0.298
	1.745	2.233	1.709	1.606	0.683	0.877	0.646	0.330
K		1.245	1.680	1.307	1.256	0.693	1.082	0.453
		2.013	2.150	1.428	1.204	0.588	0.856	0.351
		1.785	1.968	1.359	1.206	0.624	0.939	0.390
L			1.353	1.471	1.173	1.311	1.118	0.400
			1.553	1.503	1.065	1.084	0.881	0.309
			1.458	1.467	1.087	1.159	0.967	0.344
M				0.751	1.198	1.008	0.731	
				0.707	1.028	0.814	0.573	
				0.715	1.080	0.879	0.631	
N					0.682	1.000	0.456	
					0.556	0.786	0.353	
					0.599	0.864	0.392	
O		T = 0 s				0.541		
		T = 0.133 s				0.419		
		T = 2.5 s				0.465		

Assembly Averaged Power at three states of the core (CRONOS)

Figure 11 : assembly averaged radial power